

Supporting Information

Low Temperature Dissociation of CO on Manganese Promoted Cobalt(poly)

Ryan A. Ciufu^{†‡}, Sungmin Han[†], Michael E. Floto[†], Graeme Henklman^{†‡}, C. Buddie Mullins^{*†§}

[†] Department of Chemistry, University of Texas at Austin, Austin, Texas 78712, United States

[‡] The Oden Institute for Computational Engineering and Science, University of Texas at Austin, Austin, Texas 78712, United States

[§] McKetta Department of Chemical Engineering, Texas Materials Institute, Center for Electrochemistry, University of Texas at Austin, Austin, Texas 78712, United States

Experimental Methods.

All experiments were performed in a supersonic molecular beam apparatus under ultrahigh vacuum conditions with a base pressure of 1×10^{-10} Torr, which has been described in detail in a previous paper.¹ In this study, various coverages of Mn were deposited onto a $10 \times 15 \times 1$ mm Co(poly) substrate which was spot welded to cobalt wires for heating (direct current) and cooling. Mn deposition was performed with the sample at 100 K and subsequently flashed to 900 K at 5 K/s to anneal and alloy the sample. Monolayer (ML) deposition was calibrated with a quartz crystal microbalance (QCM) assuming the radius of Mn as 1.27 Å. All gas molecules were delivered via a neat molecular beam at room temperature (incidence energy of ~0.1 eV), which allows for the accurate control of the amount of adsorbed target molecules on the surface. Temperature programmed desorption (TPD) was adopted to analyze the gas phase species that evolved from the various Mn/Co surfaces. Reflection absorption infrared spectroscopy (RAIRS) was performed at 100 K to study surface intermediates. Prior to every experiment, the sample was cleaned with Ar⁺ sputtering and annealing to 950 K. Multiple sputter/anneal cycles were used to remove as much bulk carbon as possible from the substrate.¹⁷ The cleanliness of the surface was verified with Auger electron spectroscopy (AES) before each experiment.

Experimental Apparatus. In brief, the apparatus is capable of generating two separate molecular beams, and is equipped with a Bruker Tensor 27 Fourier transform infrared spectrometer with a mercury-cadmium telluride (MCT) detector, a Physical Electronics 10-500 Auger electron spectrometer (AES), and an Extrel C-50 quadrupole mass spectrometer (QMS). A rectangular polycrystalline cobalt sample (15 mm x 10 mm x 0.7 mm) is held in vacuum by spot-welded cobalt wires attached to a liquid nitrogen reservoir to both cool and resistively heat the sample. The sample temperature was monitored by a K-type thermocouple that was spot welded

to the back of the sample. The cobalt sample was cleaned with Ar^+ sputtering and then annealed to 950 K. We employed an Omicron EFM 3i electron-beam evaporator to evaporate Mn (ESPI Metals, 99.8%) onto our Co(poly) sample. Manganese deposition was calibrated with a quartz crystal microbalance (QCM) and controller (Maxtek Inc.) with the assumption of a thickness of 1 monolayer (ML) of Mn as 2.54 Å. Mn evaporation was performed with the Co(poly) sample held at 100 K. Following evaporation, the sample was annealed to 900 K at 5 K/s. AES was performed with a beam voltage of 3 kV.

CO Surface Coverage Determination. For a typical K+W experiment, the sample was exposed to a molecular beam of CO at 100 K (Figure S1a). The total uptake of CO was determined by integrating the area under the curve, from the beginning of the exposure, until saturation (Figure S1b).

DFT Calculations. We performed spin-polarized DFT calculations using the Vienna ab initio Simulation Package (VASP).³⁻⁶ The projector augmented wave (PAW) framework was used to treat interactions between the core and valence electrons.^{7,8} Electronic exchange and correlation were described with the Generalized Gradient Approximation (GGA) - Perdew-Burke-Ernzhof (PBE) functional.^{9,10} The systems were modelled as 4-layer slabs with a 2 x 2 supercell. The bottom two layers were fixed in their bulk positions, and the top two layers were allowed to relax freely. The slabs were separated in the z-direction by a vacuum layer of 10 Å. Optimized lattice parameters of $a = 2.49$ Å and $c = 4.03$ Å were determined and are in agreement with experimental values of 2.50 Å and 4.06 Å, respectively.¹¹ A cutoff energy of 450 eV was used for all calculations. The Brillouin zone was sampled with a 7 x 7 x 1 mesh using the Monkhorst-Pack scheme.¹² Methfessel-Paxton¹³ smearing was employed with a width of 0.2 eV. The convergence criteria for the electronic structure and atomic geometry were set to 10^{-5} eV and $0.05 \text{ eV} \cdot \text{Å}^{-1}$, respectively.

For all Mn/Co models, CO adsorption was found to be most stable on three-fold hollow sites, in agreement with previous studies.¹⁴ For the dissociated state, most stable structures were found with carbon bound to a hcp hollow site, and oxygen bound to a FCC hollow site, as seen previously for Co(0001) systems.^{15,16}

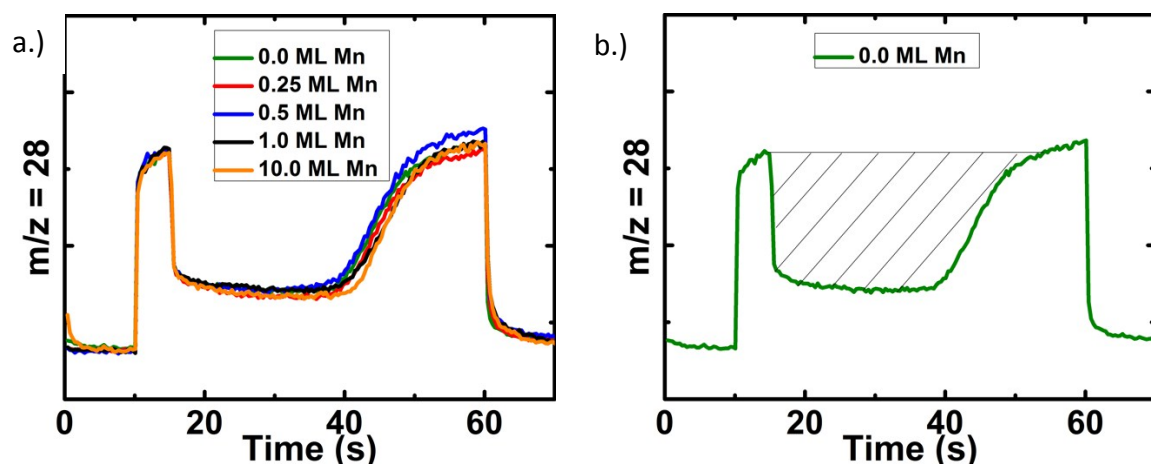


Figure S1. a.) King and Wells uptake curves for Mn/Co surfaces. b.) Schematic depicting the integrated area (hashed area) to quantify total CO uptake used in Figure 1a inset.

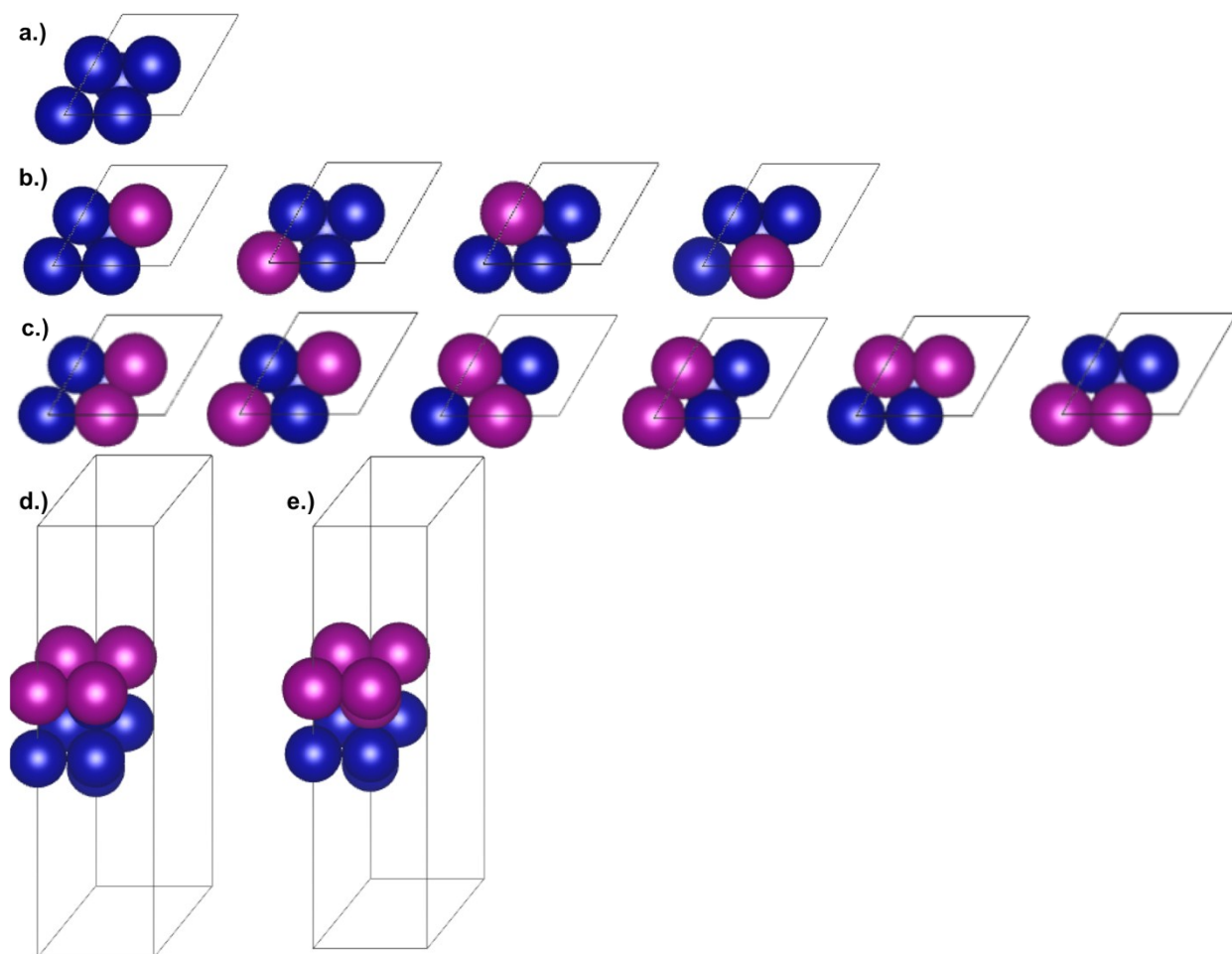


Figure S2. Illustrations of Mn/Co surfaces for DFT calculations. a.) 0 ML Mn/Co structure. b.) 0.25 ML Mn/Co structures. c.) 0.5 ML Mn/Co structures. d.) 1.0 ML Mn/Co structure. e.) 2.0 ML Mn/Co structure. blue = Co, purple = Mn

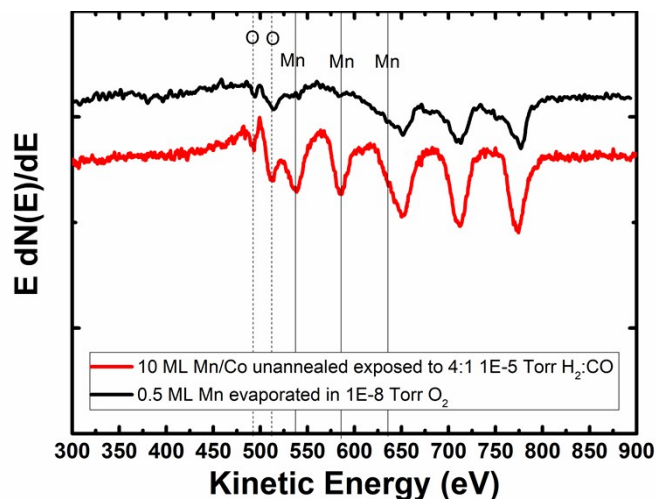


Figure S3. Auger spectrum of an unannealed 10 ML Mn/Co after exposure to $2\text{E-}6$ Torr CO and $8\text{E-}6$ Torr H_2 at 575 K for 10 minutes (red curve), and 0.5 ML Mn/Co evaporated in $1\text{E-}8$ Torr O_2 . Oxygen features are seen in both spectra.

Determination of the Metallic Nature of Mn.

We performed studies on two oxidized $\text{Mn}_x\text{O}_y\text{-Co}$ samples to better understand the nature of the Mn in our system. Specifically, one sample was prepared by exposure of 10 ML of un-annealed Mn/Co to a mixture of $2\text{E-}6$ Torr CO and $8\text{E-}6$ Torr H_2 for 10 minutes at 575 K to make a $\text{Mn}_x\text{O}_y\text{-Co}$ sample, and the other was prepared by evaporation of 0.5 ML Mn in $1\text{E-}8$ Torr of O_2 to make a $\text{Mn}_x\text{O}_y\text{-Co}$ sample. Auger of the $\text{Mn}_x\text{O}_y\text{-Co}$ samples show clear oxide features that are not present in the Mn/Co samples (nor in the post TPD Mn/Co samples, Figure 3). Additionally, no oxide feature is seen by AES after exposing a clean Co(poly) surface to the same conditions as the 0.5 ML Mn evaporated in $1\text{E-}8$ Torr O_2 sample (Figure S3 black curve). This gives additional evidence that Mn_xO_y is forming and not Co_xO_y . Upon heating of the $\text{Mn}_x\text{O}_y\text{-Co}$ samples, we also are able to detect the trace desorption of $m/z^+ = 55$ from our $\text{Mn}_x\text{O}_y\text{-Co}$, but not from our Mn/Co samples. $M/z^+ = 55$ is indicative of desorption of $\text{Mn}_x\text{O}_y\text{-Co}$ (most likely MnO_2 due to its low melting point and high likelihood of formation in un-reduced catalysts).¹⁷ From these findings, and our RAIRS findings showing no interactions between CO and Mn_xO_y , we conclude that our system has predominantly metallic Mn.

References

- 1 D. W. Flaherty, N. T. Hahn, D. Ferrer, T. R. Engstrom, P. L. Tanaka and C. B. Mullins, *J. Phys. Chem. C*, 2009, **113**, 12742–12752.
- 2 G. Bardi, U.; Tiscione, P.; Rovina, *Appl. Surf. Sci.*, 1986, **27**, 299–317.
- 3 G. Kresse and J. Hafner, *Phys. Rev. B*, 1993, **47**, 558.
- 4 G. Kresse and J. Hafner, *Phys. Rev. B*, 1994, **49**, 14251.
- 5 G. Kresse and J. Furthmüller, *J. / Am. Water Work. Assoc.*, 1996, **6**, 15–50.
- 6 G. Kresse, J. Furthmüller, Y. J. Li, Y. J. Chen, J. C. Walmsley, R. H. Mathinsen, S. Dumoulin, H. J. Roven, S. Yip, T. Supervisor and S. Chen, *Phys. Rev. B*, 1996, **54**, 11169–11186.
- 7 G. Kresse and D. Joubert, 1999, **59**, 11–19.
- 8 P. E. Blochl, *Phys. Rev. B*, 1994, **50**, 17953–17979.

- 9 J. P. Perdew, K. Burke and M. Ernzerhof, *Phys. Rev. Lett.*, 1996, **77**, 3865–3868.
- 10 J. P. Perdew, K. Burke and M. Ernzerhof, *Phys. Rev. Lett.*, 1997, **78**, 1396.
- 11 F. Ono and H. Maeta, *Le J. Phys. Colloq.*, 1988, **49**, C8-63-C8-64.
- 12 H. J. Monkhorst and J. D. Pack, *Phys. Rev. B*, 1976, **13**, 5188–5192.
- 13 M. Methfessel and A. T. Paxton, *Phys. Rev. B*, 1989, **40**, 3616–3621.
- 14 O. R. Inderwildi, S. J. Jenkins and D. A. King, *J. Phys. Chem. C*, 2008, **112**, 1305–1307.
- 15 J. X. Liu, H. Y. Su, D. P. Sun, B. Y. Zhang and W. X. Li, *J. Am. Chem. Soc.*, 2013, **135**, 16284–16287.
- 16 B. Li, Q. Zhang, L. Chen, P. Cui and X. Pan, *Phys. Chem. Chem. Phys.*, 2010, **12**, 7848–7855.
- 17 F. Morales; D. Grandjean; F. M. F. de Groot; O. Stephan and B. M. Weckhuysen, *Phys. Chem. Chem. Phys.*, 2005, **7**, 568–572.